

AD625384

ARL 65-212
OCTOBER 1965



Aerospace Research Laboratories

EXPERIMENTAL INVESTIGATIONS OF HYPERSONIC FLOW AROUND TWO-DIMENSIONAL CIRCULAR CYLINDERS

K. H. TOKEN
H. OGURO
UNIVERSITY OF CINCINNATI
CINCINNATI, OHIO

CLEARINGHOUSE FOR FEDERAL SCIENTIFIC AND TECHNICAL INFORMATION			
Hardcopy	Microfilm	Microfiche	Other
\$2.00	\$0.50	38	03
ARCHIVE COPY			

Code 1

OFFICE OF AEROSPACE RESEARCH
United States Air Force



ARL 65-212

**EXPERIMENTAL INVESTIGATIONS OF HYPERSONIC FLOW
AROUND TWO-DIMENSIONAL CIRCULAR CYLINDERS**

**K. H. TOKEN
H. OGURO**

**UNIVERSITY OF CINCINNATI
CINCINNATI, OHIO**

OCTOBER 1965

**Contract AF 33(616)-8453
Project 7064**

**AEROSPACE RESEARCH LABORATORIES
OFFICE OF AEROSPACE RESEARCH
UNITED STATES AIR FORCE
WRIGHT-PATTERSON AIR FORCE BASE, OHIO**

FOREWORD

This interim technical report was prepared by the University of Cincinnati Hypersonic Aerodynamics Research Staff on Contract AF 33(616)8453, entitled, "Experimental Aerothermodynamic Investigations," for the Aerospace Research Laboratories, Office of Aerospace Research, United States Air Force. The work reported herein was accomplished under Project 7064, "Aerothermodynamic Investigations in High-Speed Flow," during the period between October 1963 and June 1964, and is the second of a two report series dealing with the subject. Colonel Andrew Boreske, Jr., Deputy Commander of the Aerospace Research Laboratories, served as Project Monitor for this work.

ABSTRACT

This paper describes an experimental investigation of the flow phenomena about a two-dimensional circular cylinder in a hypersonic stream. The purpose of the investigation was to record properties of the flow regions which have a direct effect on the wake behind a two-dimensional circular cylinder. All data were obtained at a nominal Mach number of 14 and a stagnation temperature of 1800°R. The total pressure settings were between 600 and 2000 psia, although the majority of the data was taken at 1000, 1200, 1400, or 1600 psia. Model diameters varied from 1/4 to 3/4 inch, however tests about 3/8 and 1/2 inch diameter models were most common. Data concerning pressure distributions at the body, in the base flow region and near wake were obtained. In addition, some qualitative results were obtained with the hot wire anemometer at the body surface.

TABLE OF CONTENTS

SECTION		PAGE
I	INTRODUCTION	1
II	EXPERIMENTAL METHOD	2
	MODEL SUPPORT MECHANISM	2
	EXPERIMENTAL MODELS	3
	TOTAL PRESSURE PROBES	6
	INSTRUMENTATION AND RECORDING EQUIPMENT	7
	DATA REDUCTION	9
III	DISCUSSION OF RESULTS	10
	SURFACE PRESSURE DISTRIBUTIONS	10
	BASE FLOW AND NEAR WAKE PRESSURE	11
	NEAR WAKE PITOT PRESSURE PROFILES	12
	HOT WIRE ANEMOMETER RESULTS IN THE BOUNDARY LAYER	12
IV	CONCLUSIONS	14
V	REFERENCES	15

LIST OF ILLUSTRATIONS

Figure No.		Page No.
1	Schematic Diagrams of the Model Positioning System	17
2	Experimental Determination of the Proper Pressure Orifice Size	18
3	Schematic Diagram of the Surface Pressure Measuring Circuit	19
4	Schematic Diagram of the Base Flow and Near Wake Pressure Model	20
5	The Surface Hot wire Model	21
6	Total Pressure Probe Design	22
7	Reservoir Pressure vs. Foreward Stagnation Point Pressure	23
8	Surface Pressure Distribution on Cylindrical Model	24
9	Surface Pressure Distribution in the Base Flow Region	25
10	Centerline Pressure Variation Downstream of the Model	26
11	Pitot Pressure Profiles in the Near and Far Wake	27
12	Hot Wire Anemometer Results - Voltage vs. Angular Position	28

NOMENCLATURE

P	Pressure
V	Voltage
α	Angle measured from forward stagnation point
S	Distance along the outer edge of the boundary layer, measured from forward stagnation point
R_e	Free stream Reynolds number based on model diameter
d	Body diameter
x	Axial distance downstream measured from center of model
y	Distance measured transverse to free stream direction from body centerline

SUBSCRIPTS

T	Total conditions
s	Stagnation point conditions
α	Model surface conditions
T_2	Stagnation conditions in wake

I INTRODUCTION

Based on the results of Reference 1, which embodies the Schlieren analysis of the flow phenomena about a two-dimensional circular cylinder in a Mach 14 flow, this report describes measurements of a quantitative nature pertaining to the same problem. It is suggested that the reader review Reference 1 before engaging this report. One result of that previous work was the determination of two distinctly different flow patterns occurring chronologically during each tunnel run. The second of these flow patterns represents a majority of the run duration and, based on the Schlieren analysis, promised to yield data of much greater value to the hypersonic wake problem than the initial flow pattern. Therefore, only data obtained during the second flow regime is presented in this report. The flow pattern of the second flow regime was characterized by a wake neck region which was geometrically invariant with respect to Reynolds Number variation. This geometrical invariance is in direct conflict with other results published on the hypersonic wake problem. It was suggested in Reference 1 that there was the possibility that the second flow pattern established contains turbulent flows upstream of the flow neck.

The purpose of this report was to determine conclusively the nature of the second flow regime and to obtain data in that regime. Toward these goals, several experimental techniques were employed. Successful measurements were obtained of surface pressure distributions and pressure distributions in the vicinity of the body. Limited hot wire anemometer results on the model surface were also obtained. Other techniques, including hot wire anemometer measurements in the near wake and the glow discharge flow visualization technique, were not promising.

Manuscript released July 1965 by the authors for publication as an ARL technical documentary report.

The experimental program was conducted in the twenty-inch diameter hypersonic wind tunnel located at the Aerospace Research Laboratories at a nominal Mach Number of 14. The models employed were similar to those used for the Schlieren analysis (Reference 1), with the exception that they were now modified to accommodate instrumentation and sensing elements. Quantitative data were contained at the mid-span, where end effects were deemed negligible due to the large aspect ratios of the models.

II EXPERIMENTAL METHOD

The twenty-inch diameter hypersonic tunnel located at the Aerospace Research Laboratories, is of the axisymmetric, open jet, and blow down type. Detailed descriptions of this facility can be found in References 2 through 5.

All tests were conducted at a constant total temperature of 1900°R (nominal at throat), and a Mach number of 14. Total pressure was varied from 600 to 2000 psia and model diameters were 1/8, 3/16, 1/4, 5/16, 3/8, 1/2, or 3/4 inch. This represents a change in free stream Reynolds number based on model diameter (Re_d) from 0.322×10^4 to 6.44×10^4 . Most tests, however, were performed with 3/8 or 1/2 inch diameter models at 1000, 1200, 1400, or 1600 psia, which corresponds to a Reynolds number variation (Re_d) from 1.61×10^4 to 3.43×10^4 .

MODEL SUPPORT MECHANISM

Experimental models were supported in much the same manner as those employed in Reference 1. In particular, those models which did not require angular orientation were supported in exactly the same manner. All other models, including the surface pressure model,

the rearward facing probe model, and the hot wire anemometer model required a redesigned support mechanism. This redesign constituted the attachment of a drive mechanism to the original support structure. One "T" plate was made to house this gear train which was driven by a Bodine, reversible capacitance type, 1/20 horsepower motor. Requirements on the drive mechanism were remote control, accurate position indication, and sufficient clearance in the region of the model to allow the passage of Schlieren light for monitoring the flow pattern. These conditions were met as shown on Figure 1. As shown, power at 27 R.P.M. was transmitted through a 6:1 gear ratio, giving model rotation of 4.5 R.P.M. in a circumferential direction. Tests on the positioning mechanism indicated a linear output, reproducible to within 8 minutes of arc. Schematic diagrams of the model positioning mechanism and electrical circuits of the drive mechanism and position indicator are given in Figure 1.

EXPERIMENTAL MODELS

The experimental program employed several types of models. Each of these models is discussed below.

Surface Pressure Models

The orifice size of a surface pressure model must be relatively small so that the pressure measured approaches a point measurement. This becomes increasingly important in regions wherein the surface pressure gradients are steep, since in these regions the integrity of the readings becomes questionable. There is, however, another restriction on orifice size when short run time facilities are employed. Time lag phenomena in the pressure measuring circuit may exclude the efficient use of the facility, or in the limit, prevent measurements from being taken. Hence, tests were conducted to find the optimum orifice diameter. Surface pressure models employed for these tests were 3/8 or 1/2 inch diameter. Based on tests of three

orifice diameters; 0.030, 0.015, and 0.009 inch on 3/8 inch diameter models, an orifice size of 0.013 inch diameter was found to be desirable. In addition, it can be attained with a common drill size. Results of the orifice size tests are shown on Figure 2. As shown, a 0.013 inch diameter orifice would produce adequate resolution in measurement. Inherent with this size port however, large time lag problems occurred. The time lag phenomenon was eradicated by using a number of 0.013 inch diameter orifices to feed the larger diameter tube which connected the orifices to the pressure transducer. A total of eight orifices were employed. The determination of the number of orifices was based on assumptions of Poiseuille type flow in the orifices, and a balance of the resistance to flow between the orifice and transducer feed tube portions of the pressure measuring circuit. It should be recognized that this results in a conservative estimate of the number of orifices required. Figure 3 illustrates the model and the remainder of the pressure measuring circuit. The eight ports were arbitrarily spaced ten diameters apart, from center to center, so as not to interfere with one another.

Base Flow and Near Wake Pressure Model

Figure 4 illustrates the construction details and tunnel orientation of this model. As indicated, the probe from this model is pointed downstream in an attempt to measure pressures very closely related to static pressure. The model oriented in such a manner was rotated in order that the centerline pressure could be obtained by symmetry. Probe lengths of 0, 1/4, 3/4, 1, 1 1/4, 1 1/2, and 1 3/4 inches from the body were deployed behind a 1/2 inch diameter model. These resulted in nondimensionalized distances of s/d equal to 1, 2, 2.5, 3, 3.5, and 4.0. It should be recognized that the pressure measured in such a fashion is dependent on two entirely different flows.

In the region where the flow is returning to the model, or all points between the model and the wake neck region, the probe reacts as a subsonic pitot tube in a region of very low dynamic pressure. Evidence that the dynamic pressure is low can be seen on the surface pressure profiles shown on Figure 9, which is presented later in the present report. In this subsonic region of low dynamic pressure, the probe transmits a pressure very close to the static pressure. Downstream of the wake neck the probe experiences first subsonic then supersonic and finally hypersonic Mach numbers. This change in Mach number is inflicted at progressively larger x/d values downstream by the acceleration of the viscous wake due to interaction with the relatively high Mach number inviscid wake. Again, in these flow regimes the pressure measured is not too much different from static pressure. It should be noted that in the region between the model and the wake neck the measured pressure is somewhat higher than local static pressure and downstream of the wake neck the measured pressure is somewhat lower than local static pressure.

Hot Wire Anemometer Model

This model, as shown on Figure 5, was basically a $3/8$ inch O.D., $3/16$ inch I.D. stainless steel cylinder fitted with the necessary instrumentation components which would allow a hot wire surface investigation. In common with all other models, this model exceeded in length the span required to extend beyond the nozzle exit diameter on both ends where it was supported by the modified "T" plates. In order to minimize heat conduction losses from the hot wire, 0.0001 inch diameter Wollaston processed wire was spot welded across 0.011 inch diameter Michrome wire posts, which were cemented in place 0.030 inch apart from centerline to centerline. The wire was parallel to the axis of the model. The resulting x/D ratio of the hot wire was 300 which was deemed sufficient. The actual spot weldings were accomplished using a specially designed hot wire welding fixture. Initial experiments with this model were designed such that the hot

wire would be used as a constant current device. It was planned, however, to eventually employ the model to determine mass flow profiles. Both current and voltage monitoring leads were attached to either side of the hot wire. Ideally, the joints of the current and voltage leads should be made as close as possible to the hot wire joints in order to minimize possible potential drop through lead wires due to high temperature loading. In this model these joints were approximately 0.095 inch apart, or 8.65 diameters. The entire region of the hot wire and current-voltage joints was encased in type 27-A Saurisen high temperature electrical insulated cement. The Saurisen served to hold rigid the hot wire posts and to insulate them from the metal model. Away from this region mullite ceramic spaghetti insulated the leads in the high temperature regions, while teflon spaghetti was used in more moderate environments.

TOTAL PRESSURE PROBES

Experiments which were directed toward the generation of total pressure profiles in the near wake employed stainless steel models similar to those used for the Schlieren investigation of Reference 1. These models were also supported by the simple structure discussed in Reference 1. In order to obtain adequate resolutions to define the total pressure profiles behind the relatively small diameter models, minimum possible diameter pitot tubes were required. Inherently associated with these smaller diameter pitot tubes is the time lag problem. This was overcome, however, with the probe design shown on Figure 6. As is shown in that figure, a flattened total head tube, similar to those used in boundary layer measurement, was used. The pitot probes were fitted to the vertical traverse mechanism which is a permanent part of the facility. This device allows vertical positioning within \pm 10 inches of the tunnel centerline. The position indicator on this device allows vertical positioning within 0.015 inch. Variation in distance between the probes and the model was achieved with extensions to the probes. The non-dimensionalized distance is further varied by changes in model diameter from $3/16$ to $1/2$ inch.

INSTRUMENTATION AND RECORDING EQUIPMENT

Two types of recording instruments were used during the experimental program. Analog recording was accomplished with the use of Moseley type x-y plotters. Digital records were obtained using the Microsadic data acquisition system. The Microsadic system can accept 40 input data channels and amplifies each channel independently by a pre-selected gain factor. Each of such amplified analog signals are then sampled at a rate of up to 10,000 samples per second. The data samples are then stored on magnetic tape in the binary coded decimal format. Printed results were later obtained through the use of an IBM7094 computer. A more detailed description of this system can be found in Reference 5. All tests employed the analog equipment, if only for purposes of monitoring the output. The digital system, however, was used only during tests wherein a more accurate record was desirable. The instrumentation and recording equipment used and their deployment are indicated in the following subsections which deal with the individual test programs.

Surface Pressure Distributions

During each test relevant to surface pressure, x-y plotters recorded surface pressure against pressure port position as the model was rotated in increments of approximately 5 degrees. Incremental model positions were needed to account for the time lag phenomena. The x-y plotters were also used to record pitot pressure vs. time, and surface pressure vs. time. These latter plots were used to correlate surface pressure to pitot pressure. The tolerance on reproducible total pressures between tunnel runs was on the order of ± 50 psia. It was imperative, therefore, to continuously monitor pitot pressure. Digital recording was also employed for these tests. In addition to affording a printed result, the Microsadic System features a digital display which can be locked on any particular input channel. This feature greatly aided in the detection of leaks in the pressure

measuring system, since the four digit display could be made to represent 5 microns Hg abs. per fourth place digit. This high sensitivity also aided in the detection of electrical grounds and other instrumentation problems.

All pressures were monitored by a Statham Model PA 27ITC, 0-1 psia transducer. Before and directly after each day's use the transducer was calibrated with respect to 0-5 mm and 0-50 mm Hg abs. Stokes gages. While dealing with the lower pressure ranges, however, these calibrations were checked before and after each tunnel run and used the system illustrated in Figure 3. In the pressure range below 5 mm Hg abs. calibration zero shifts above 20 microns Hg. abs. were not tolerated. In pressure ranges above 5 mm Hg. abs. zero shifts as high as 200 microns Hg abs. were accepted. Accumulated data, for which calibration shifts greater than those indicated above were obtained, was simply discarded.

Base Flow and Near Wake Pressure Records

This data was obtained by employing instrumentation and recording devices and practices identical to those used to obtain surface pressure data.

Near Wake Pitot Pressure Records

Again, this data was accumulated in much the same manner as the other pressure data. Exceptions to the other pressure measuring technique are that no digital recording was employed and that the pressure measuring system of Figure 3 was replaced by a direct line between transducer and orifice. Calibration was accomplished by connecting the system of Figure 3 to the pitot orifice by rubber surgical tubing. Plots of vertical position vs. pitot pressure were obtained.

Hot Wire Anemometer Records

The hot wire acting in its constant current mode of operation produced data plotted as voltage vs. angular position on the x-y plotter. Due to the relatively fast response of the hot wire, these plots were obtained while the model was rotated in a continuous manner. The hot wire current control and measurement were made by the Shapiro and Edwards' Model 50 constant current hot-wire anemometer system. The signal outputs were recorded on the Moseley x-y plotter.

DATA REDUCTION

This section deals only with pressure data, since the limited hot wire results at the body surface are of the qualitative type and therefore required no reduction or calibration adjustment.

All pressure data in the form recovered from the experiments merely represented analog voltage levels. Processing this data through the respective calibration curves resulted in the pressure sensed. Extremely linear calibration curves are characteristic of the transducer employed and thus reduced this work considerably.

Variations in the Mach number of the facility due to changes in area ratio of the nozzle caused by operation at different total pressures were reconciled using Figure 7. All data presented was normalized with respect to the forward stagnation point pressure. The stagnation point pressure shown on Figure 7 accounts for Reynolds Number effects in the nozzle of the facility as well as those affecting the pressure orifice at the forward stagnation point. Also shown on Figure 7 is the pressure predicted by normal shock theory. It is suggested that although the stagnation point pressure measured is sensitive to Reynolds number and resolution due to orifice size, it represents a better base pressure with which to normalize surface pressure data than normal shock theory (at correct Mach Number), since the pitot pressure thereby defined includes viscous effects.

III DISCUSSION OF RESULTS

In the following sections the salient features of the results obtained are discussed and compared to the results of other investigations.

SURFACE PRESSURE DISTRIBUTIONS

Approximately 320 data points obtained throughout the Reynolds number range define the plot of normalized surface pressure vs. angular position of the model shown on Figure 8. Due to the relatively small scale of Figure 8, it appears that the entire pressure distribution is independent of Reynolds number. Figure 9, which is drawn to a larger scale, illustrates a Reynolds number dependence in the base flow region or that region between separation and the rearward stagnation points. In Figure 8 the results of McCarthy, Reference 6, and of Gregorek and Korcan, Reference 7, are compared with the present data. As shown, an excellent agreement is found between McCarthy's and the present data in the region between the forward stagnation point and 90 degrees from the stagnation point. Beyond that point, the data do not agree. Dewey, Reference 8, reported experimental data in the base flow region which exactly agreed with McCarthy's, which spanned the entire region. A comparison is made in Figure 9 between Dewey's results obtained at the extremes of his Reynolds number excursion and the results obtained at the extremes of the Reynolds number range of the present tests. Dewey reported that with decreasing Reynolds number the separation point moves towards the rearward stagnation point and the rearward stagnation pressure decreases. The present data also shows the same trend. However, in the present experiment the wall static pressure around the circular cylinder shows a departure to a higher value and less pressure recovery after separation. As discussed in Reference 1 and the present report, all of the data were taken for the second flow pattern. In the second flow pattern,

the geometrical flow pattern in the base region is independent of Reynolds number with larger shear layer angle compared with the initial flow pattern (Reference 1). This fact suggests that the flow in the base region might be a turbulent flow in which a larger turbulent diffusion coefficient makes the flow relatively independent of Reynolds number. The larger value of the boundary layer thickness in the turbulent boundary layer beyond 90 degrees may cause the wall static pressure increase as compared with the laminar boundary layer in the cases of McCarthy and Dewey. In the present results, the separation point moves toward the rearward stagnation point and the difference of the pressure distribution in the base region due to Reynolds number difference is not significant when compared with the laminar case.

BASE FLOW AND NEAR WAKE PRESSURE

Figure 10 illustrates the pressure distribution obtained by the rearward facing probe. As indicated in the description of this model, the pressures sensed are not far different from static pressures. Thus, the centerline pressure distribution of Figure 10 is considered very close to the static pressure distribution. At each point downstream of the body in Figure 10, pressure measurement points cover the free stream stagnation pressures of 1000, 1200, 1400, and 1600 psia behind the 1/2 inch diameter model. This represents a Reynolds number range of $R_{ed} = 1.61 \times 10^4$ to 3.43×10^4 . Although the Reynolds number dependence on the normalized pressure readings is within 2.5 percent, the lower Reynolds number corresponds to the lower normalized pressure reading. All of these results are in agreement with the conclusion which was reported in Reference 1. Namely, the Reynolds number independence of the geometrical flow pattern leads to the result that the normalized pressure vs. normalized distance downstream falls on one unique curve.

There are two interesting points, wake neck point and peak pressure point. The pressure peak is located 1.5 diameter downstream of the wake neck defined by the Schlieren analysis of Reference 1. The increase in pressure from the wake neck may be due to the compression waves originated by the wake - wake shock interaction. Beyond the pressure peak, the expansion waves accelerate the wake flow to a certain velocity which is primarily determined by the outer inviscid wake. Such wake-wake shock interaction was proposed by Lees and Reeves, Reference 9.

NEAR WAKE PITOT PRESSURE PROFILES

Figure 11 illustrates pitot pressure profiles at $x/d = 2.375$ and $x/d = 174$. At values of x/d larger than 30, McCarthy, Reference 6, found a profile similar to the one obtained at $x/d = 174$. That is, without a viscous dip around the centerline, although in the laminar wake a viscous dip usually exists. The existence of the viscous dip may be considered as a characteristic of the laminar wake (References 6 and 10). This fact is consistent with the present results in which the wake flow is turbulent and the turbulent flow is possibly extended to the model surface. At a mean turbulent wake boundary, the probe would experience the laminar flow and turbulent flow intermittently as presented by Slattery and Clay, Reference 11.

HOT WIRE ANEMOMETER RESULTS IN THE BOUNDARY LAYER

Measurements were taken at a distance of 0.001 inch from the model surface. In this way the hot-wire itself stays in the boundary layer around the $3/8$ inch O. D. cylinder, except at the forward stagnation region. While the current of the hot-wire was kept constant, the model cylinder was rotated continuously and slowly over a 180 degree angle. Thus, the output lead voltages corresponded to the average temperature of the hot-wire. In Figure 12, two distinct

traces of the output voltage are shown for 0.436 ma and 35.23 ma current supplies to the hot-wire. For the low current supply, the hot-wire temperature may indicate a value close to the total temperature of the flow around the hot-wire. The temperature decrease towards the rearward stagnation point may explain a loss of the total temperature due to heat transfer into the model surface.

In the case of large current supply, there was noted a distinct departure from the smooth change. The hot-wire was more sensitive to flow velocity than to total temperature. As a result, the hot-wire temperature indicated an increase toward the rearward stagnation point. This may correspond to the increase of boundary layer thickness towards the rear stagnation point. The heat transfer is directed to the surrounding flow from the hot-wire surface. Within a \pm 40 degree angle around the forward stagnation point, there was a sharp jump when the hot-wire was rotated towards the rearward stagnation point. There was no jump when the hot-wire was rotated in a reverse direction. The first positive jump of hot-wire temperature may occur at the reattachment point. If this assumption is true, the cause could be the extra heat addition to the flow from the hot-wire surface, particularly when the hot-wire was rotated from the forward stagnation point. There might be a local creation of positive pressure gradient. Once a new flow pattern is established, the hot-wire voltage curve seems to follow the curve (1).

As it was reported in Reference 1, page 15, there were several similar photographs in the Schlieren pictures which were taken during the initial flow pattern period. It was clear in Figure 4 of Reference 1 that the bow shock was followed immediately by the second shock-like wave and expansion-like wave. More details about the second shock phenomena and the temperatures loading effect could be done by the simultaneous use of the hot-wire and Schlieren techniques.

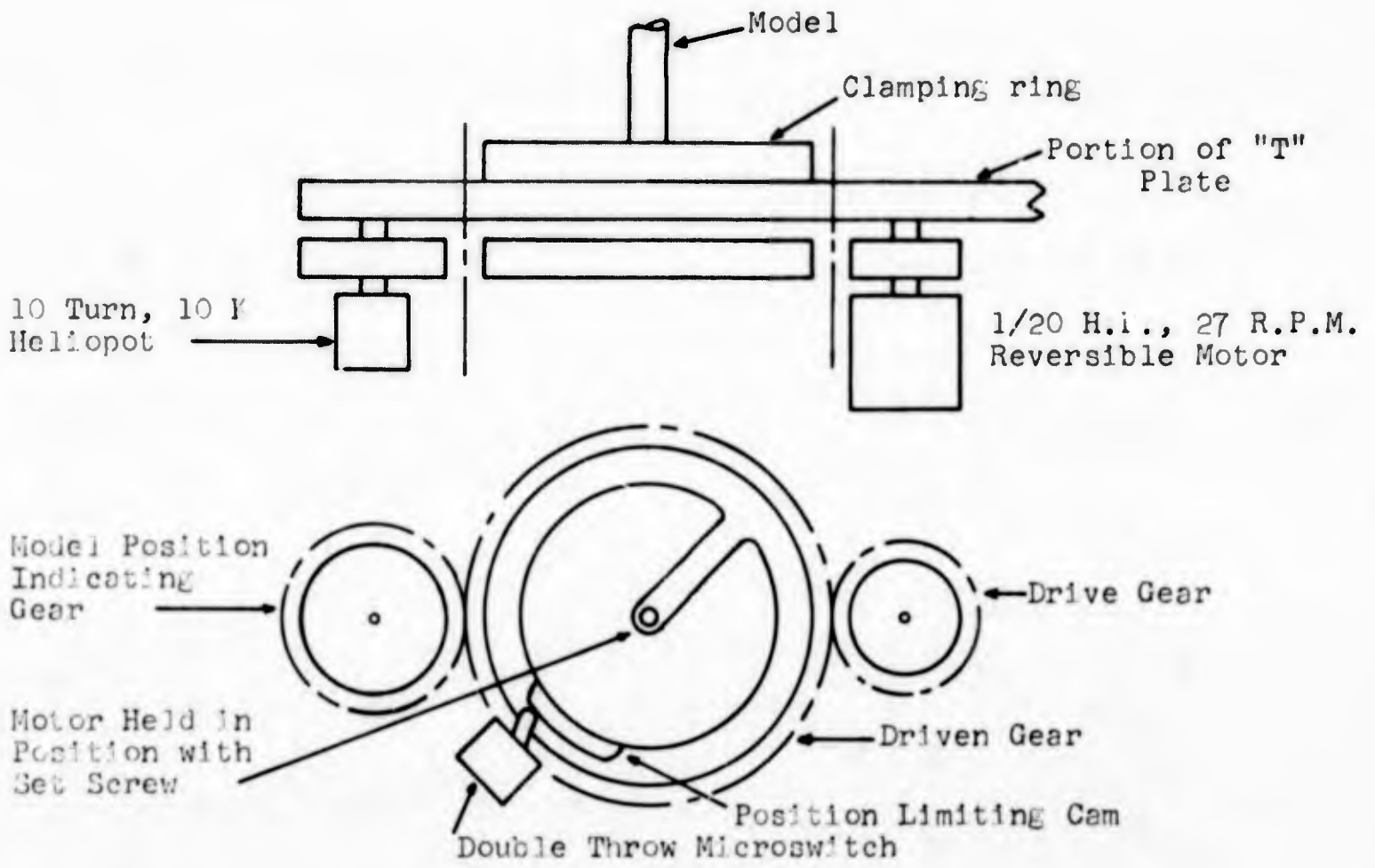
IV CONCLUSIONS

The second flow regime, which was investigated in the present report, was proven to be turbulent flow which covered an entire wake region (near and far). This is clear from the facts that the surface pressure distribution shows turbulent like behavior, the pressure distribution across the wake does not show any viscous dip around the center region, and the jump in the hot wire temperature in the front part of the model seems to be related to the existence of the second shock wave in the initial flow pattern. The concluding results in this paper should be supplemented by the results in Reference 1.

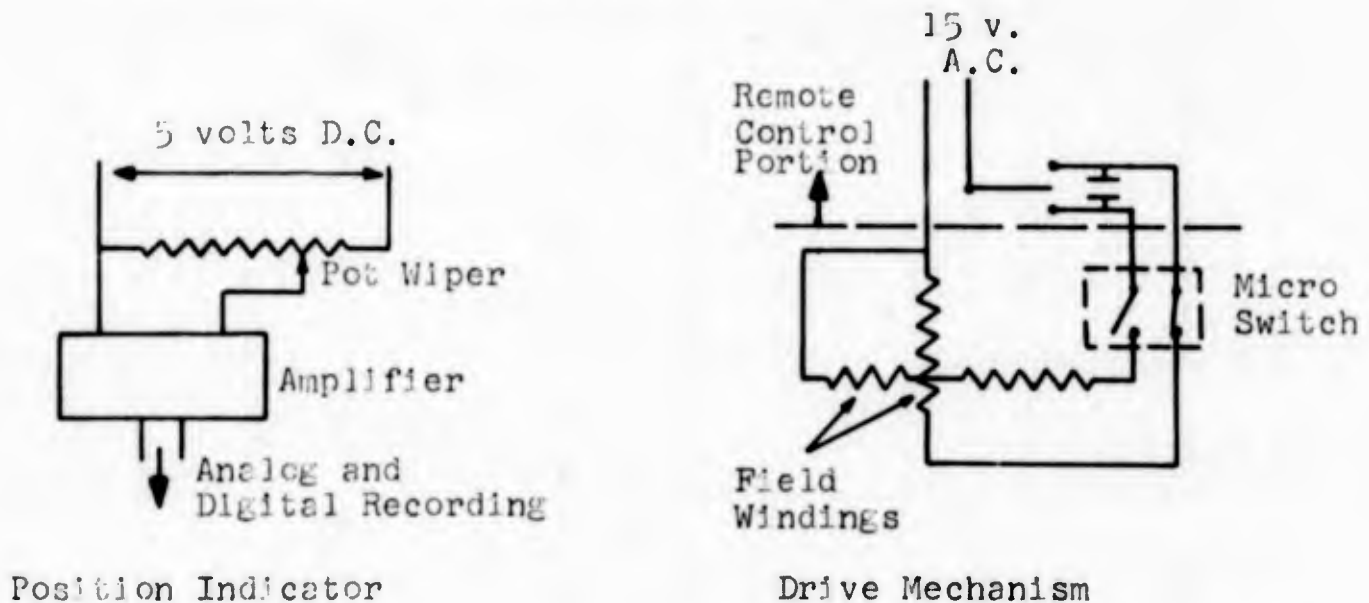
V REFERENCES

1. Token, K. H., and Oguro, H., "Schlieren Investigation of the Flow Phenomena about a Two-Dimensional Circular Cylinder in a Hypersonic Flow", ARL, 64-207, November 1964.
2. Gregorek, G. M., and Lee, J. D., "Initial Calibrations and Performance of the ARL Twenty-Inch Hypersonic wind Tunnel", ARL 62-393, August 1962.
3. Gregorek, G. M., and Lee, J. D., "Design Performance and Operational Characteristics of the ARL Twenty-Inch Hypersonic wind Tunnel", ARL 62-392, August 1962.
4. Tepe, F. R., Brown, D. L., Token, K. H., Hoelmer, w., "Theoretical Operating ranges and Calibration Results of the ARL Twenty-Inch Hypersonic wind Tunnel", ARL 63-189, October 1963.
5. Brown, D. L., Token, K. H., Hoelmer, w., and Tepe, F. R., "Instrumentation and Recording Equipment Used in Conjunction with the ARL Twenty-Inch Hypersonic wind Tunnel", ARL 63-162, September 1963.
6. McCarthy, J. F., Jr., "Hypersonic wakes", Hypersonic Research Project Memo. No. 67, GALCIT, July 2, 1962.
7. Gregorek, G. M., and Korkan, "An Experimental Observation of the Mach-and Reynolds-Number Independence of Cylinders in Hypersonic Flow", AIAA Journal, Vol. I, No. I, January 1963.
8. Dewey, C. F., Jr., "The Near wake of a Blunt Body at Hypersonic speeds", AIAA Aerospace Sciences Meeting, New York, January 20-22, 1964, Preprint No. 64-43.

9. Lees, L., and Reeves, B. L., "Supersonic Separated and Reattaching Laminar Flows: i. General Theory and Application to Adiabatic Boundary Layer - Shock Wave Interactions", AIAA Aerospace Sciences Meeting, New York, January 20-22, 1964, Preprint No. 64-4.
10. Kendall, J. M., Jr., "Experimental Study of Cylinder and Sphere Wakes at a Mach Number of 3.7". JPL Technical Report No. 32-363, 1962.
11. Slattery, R. E., and Clay, E. G., "The Turbulent Wake of Hypersonic Bodies," American Rocket Society 17th Annual Meeting, Los Angeles, California, 1962.



a. Schematic of Model Positioning Device



b. Electrical Schematic of Drive Mechanism and Position Indicator

FIGURE 1 - SCHEMATIC DIAGRAMS OF THE MODEL POSITIONING SYSTEM

FIGURE 2 - EXPERIMENTAL DETERMINATION OF ORIFICE SIZE

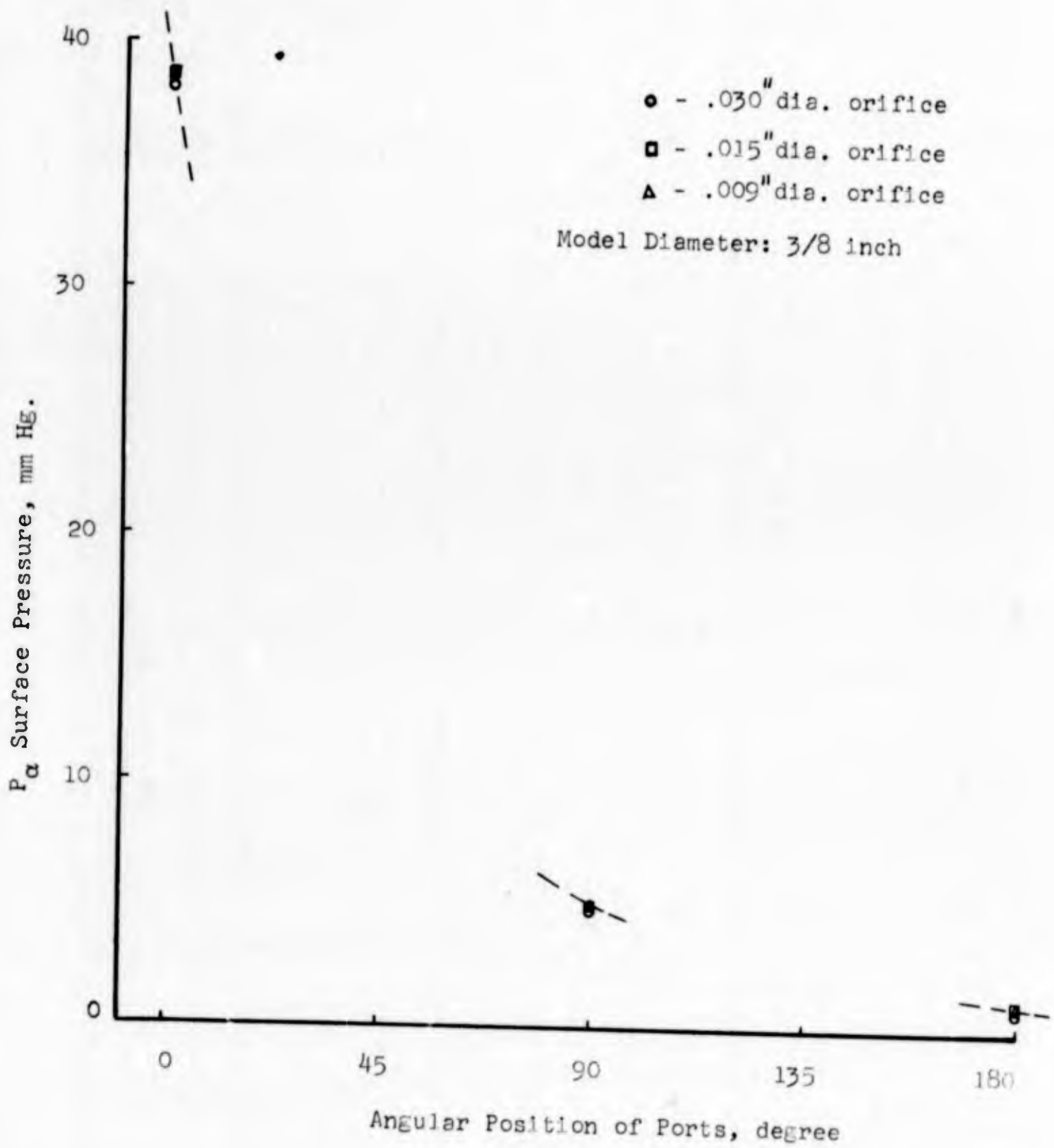
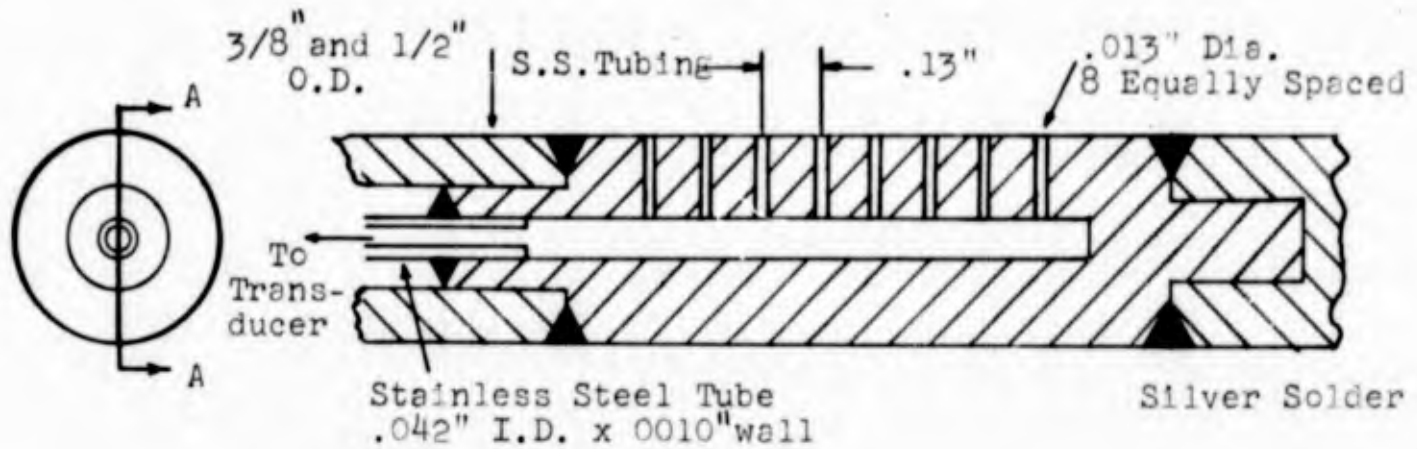
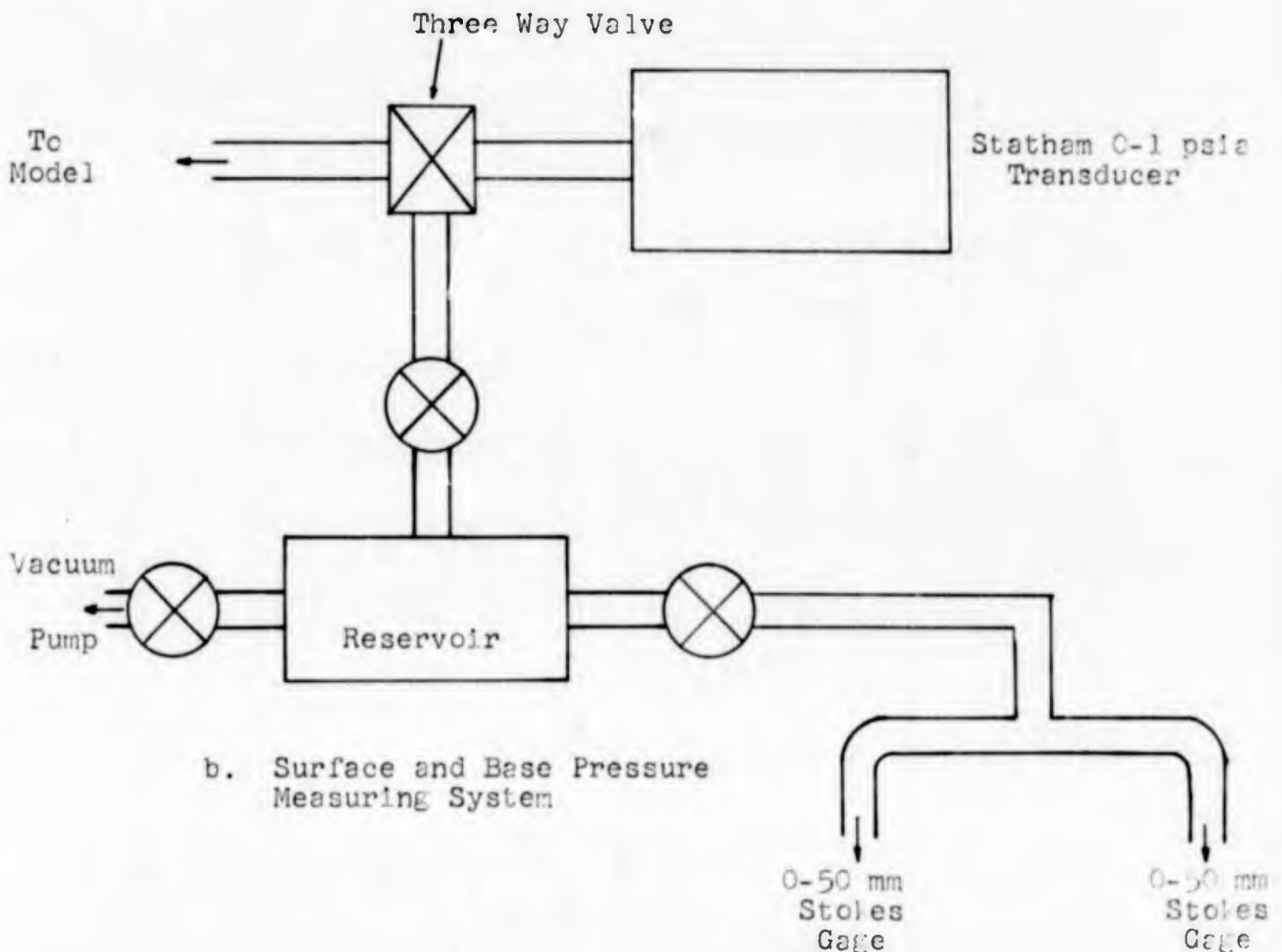


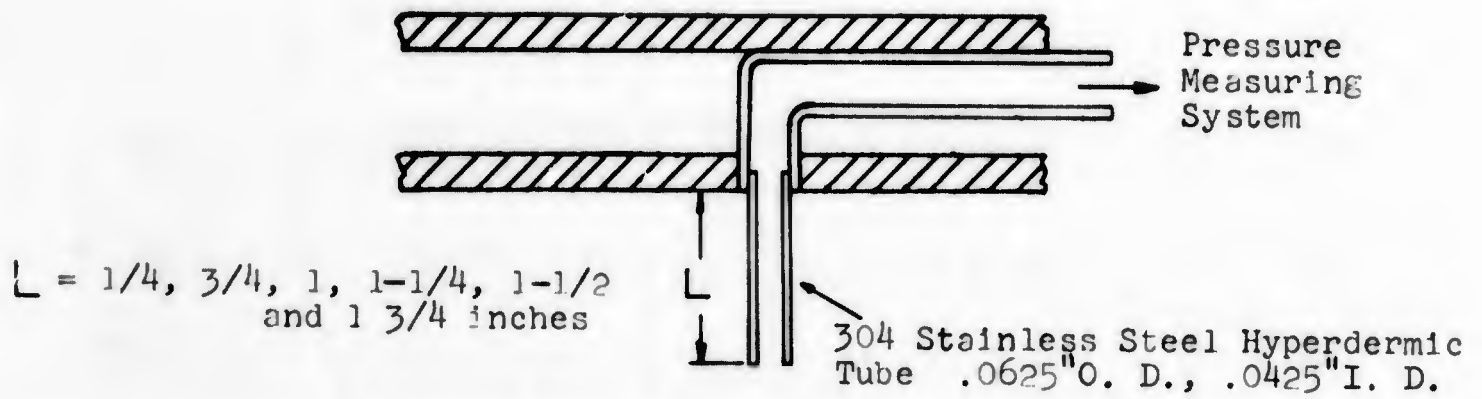
FIGURE 3 - SCHEMATIC DIAGRAM OF THE SURFACE PRESSURE MEASUREMENT CIRCUIT



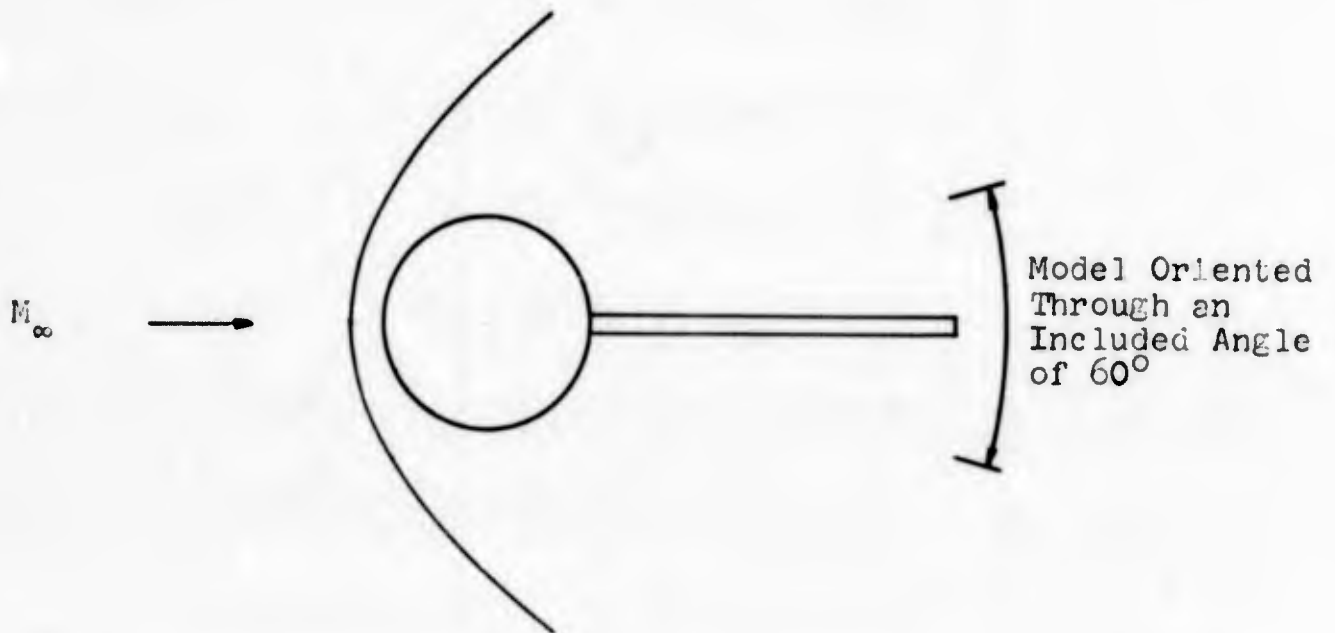
a. Surface Pressure Model



b. Surface and Base Pressure Measuring System



a. Rearward Facing Base Flow Probe



b. Orientation of Rearward Facing Probe

FIGURE 4 - SCHEMATIC DIAGRAM OF THE BASE FLOW AND NEAR WAKE PRESSURE MODEL

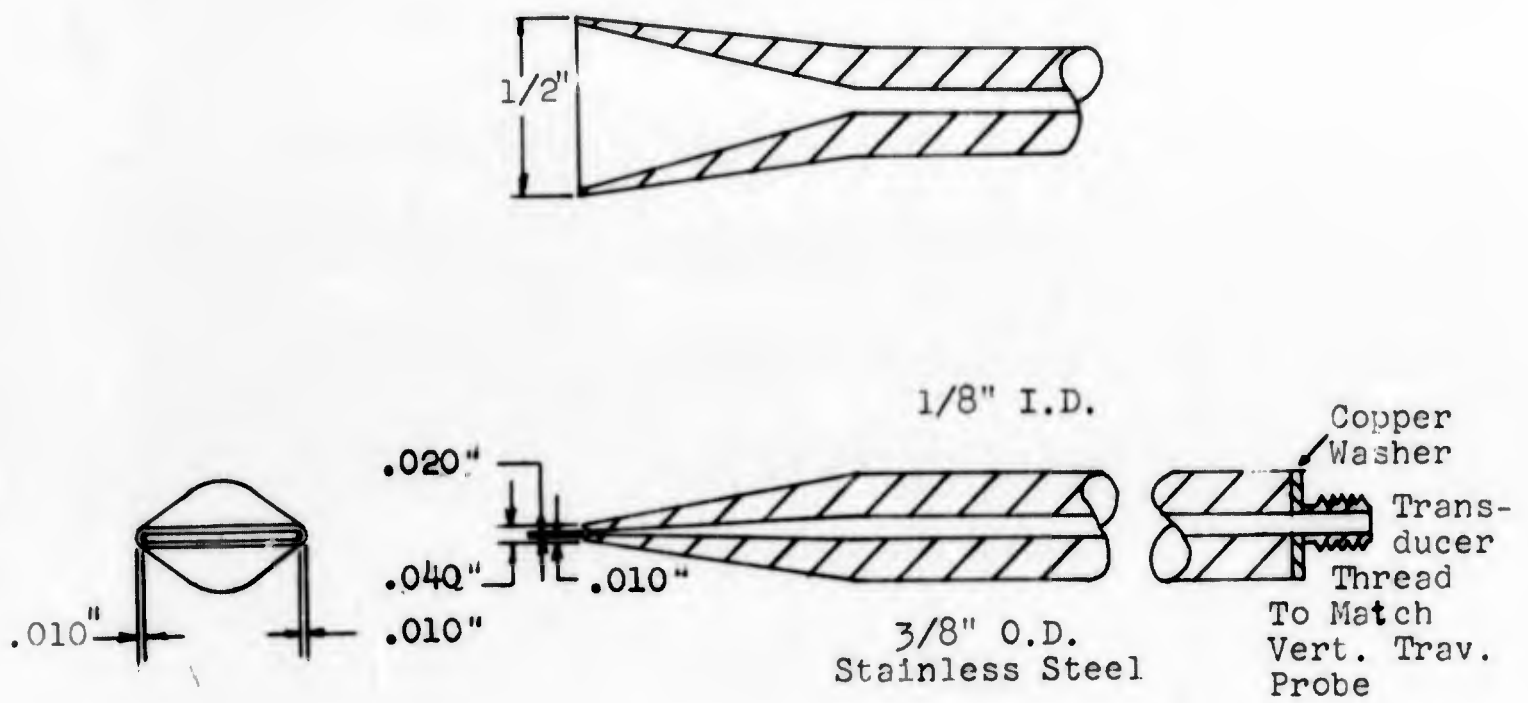


FIGURE 6 - TOTAL PRESSURE PROBE DESIGN

P_s Forward Stagnation Point Pressure, mm Hg.

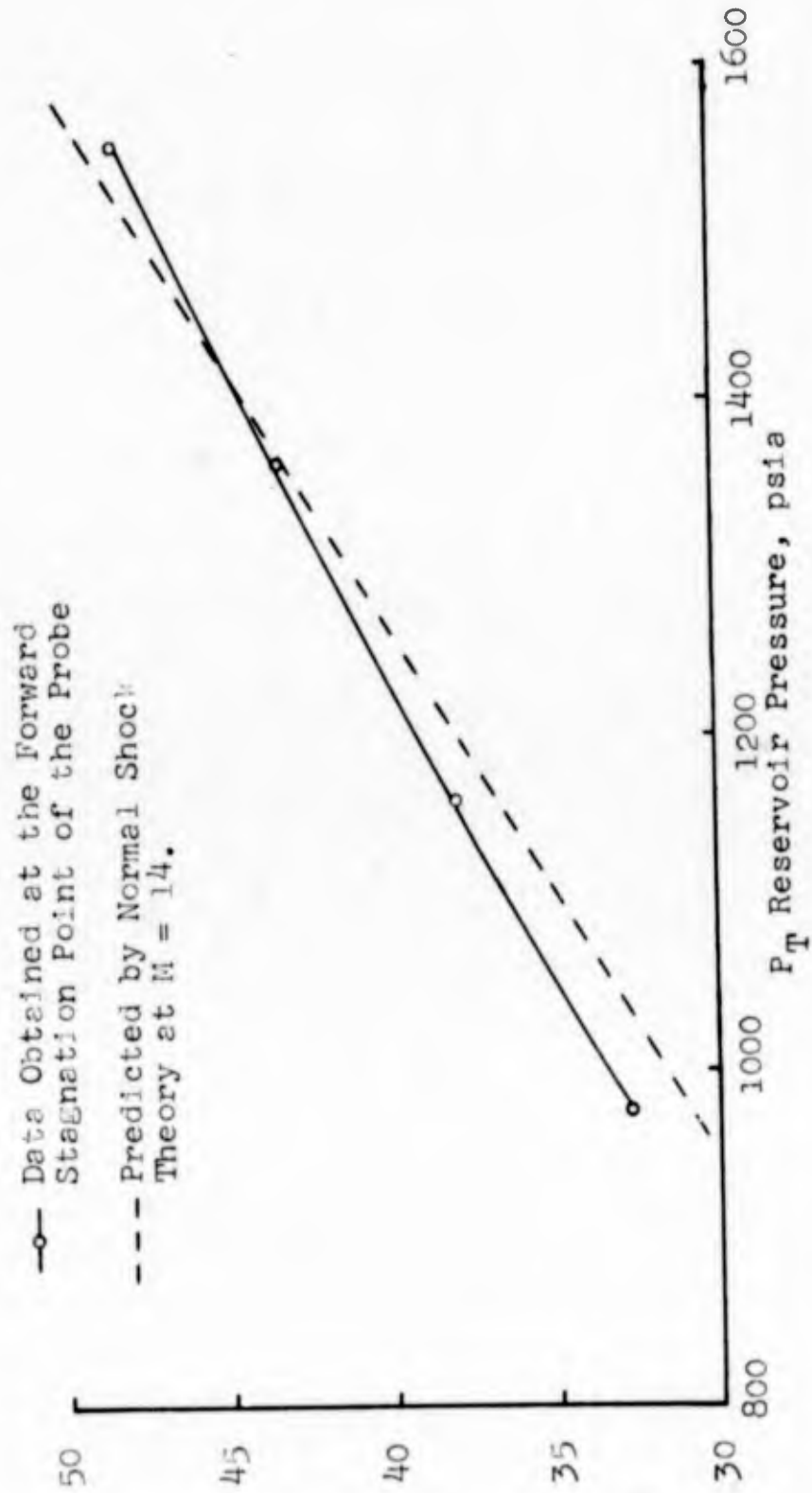


FIGURE 7 - RESERVOIR PRESSURE VS. FORWARD STAGNATION POINT PRESSURE

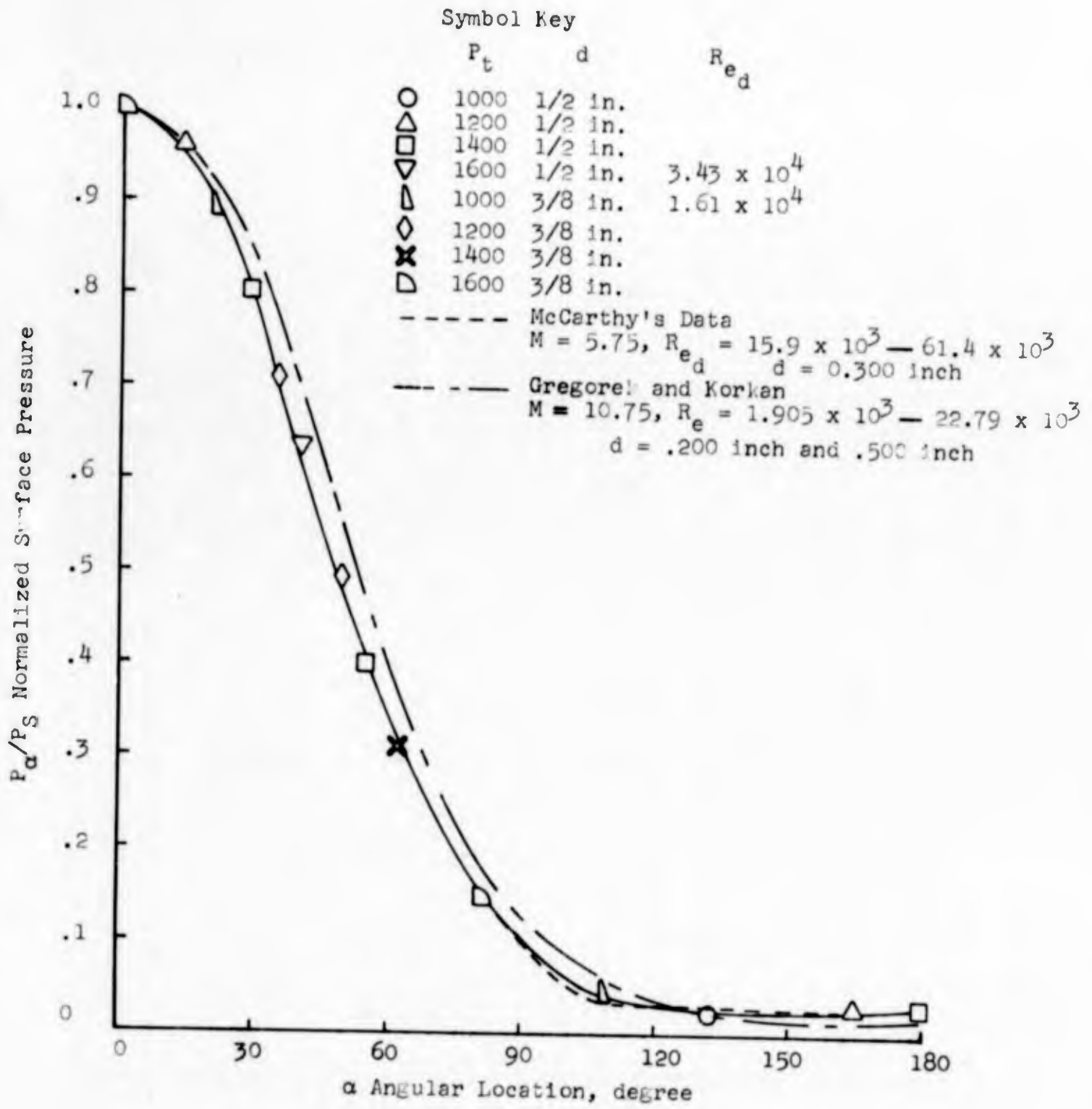


FIGURE 8 - SURFACE PRESSURE DISTRIBUTION ON CYLINDER MODEL

FIGURE 9 - SURFACE PRESSURE DISTRIBUTION IN THE
BASE FLOW REGION

$\circ - R_{ed} = 2.148 \times 10^4$ $M = 14$
 $\square - R_{ed} = 3.44 \times 10^4$ $d = 0.5''$

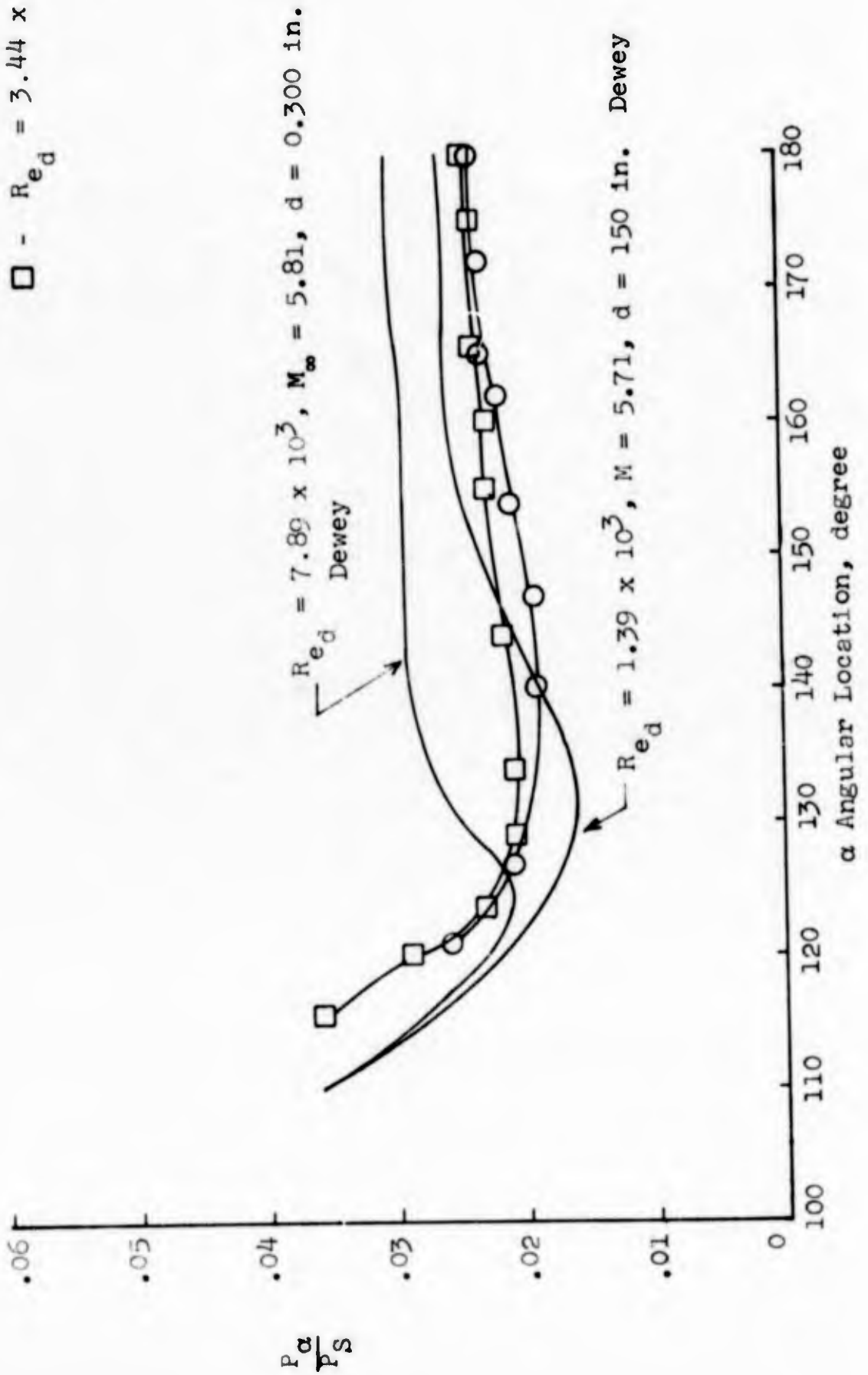
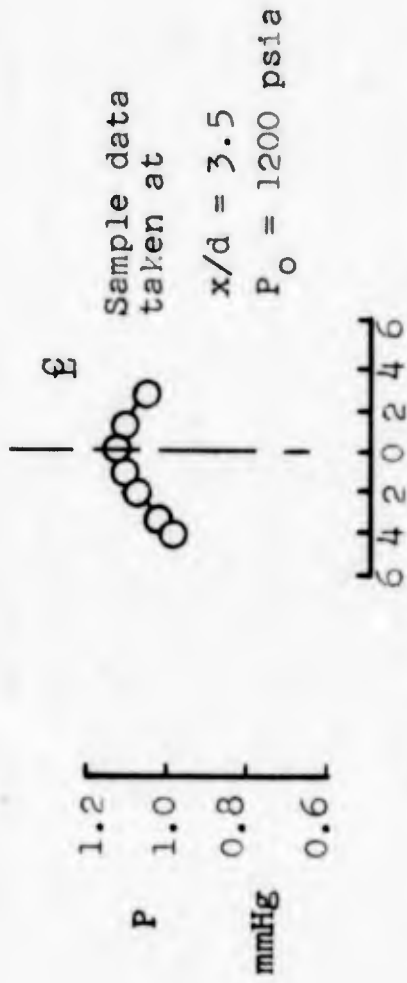
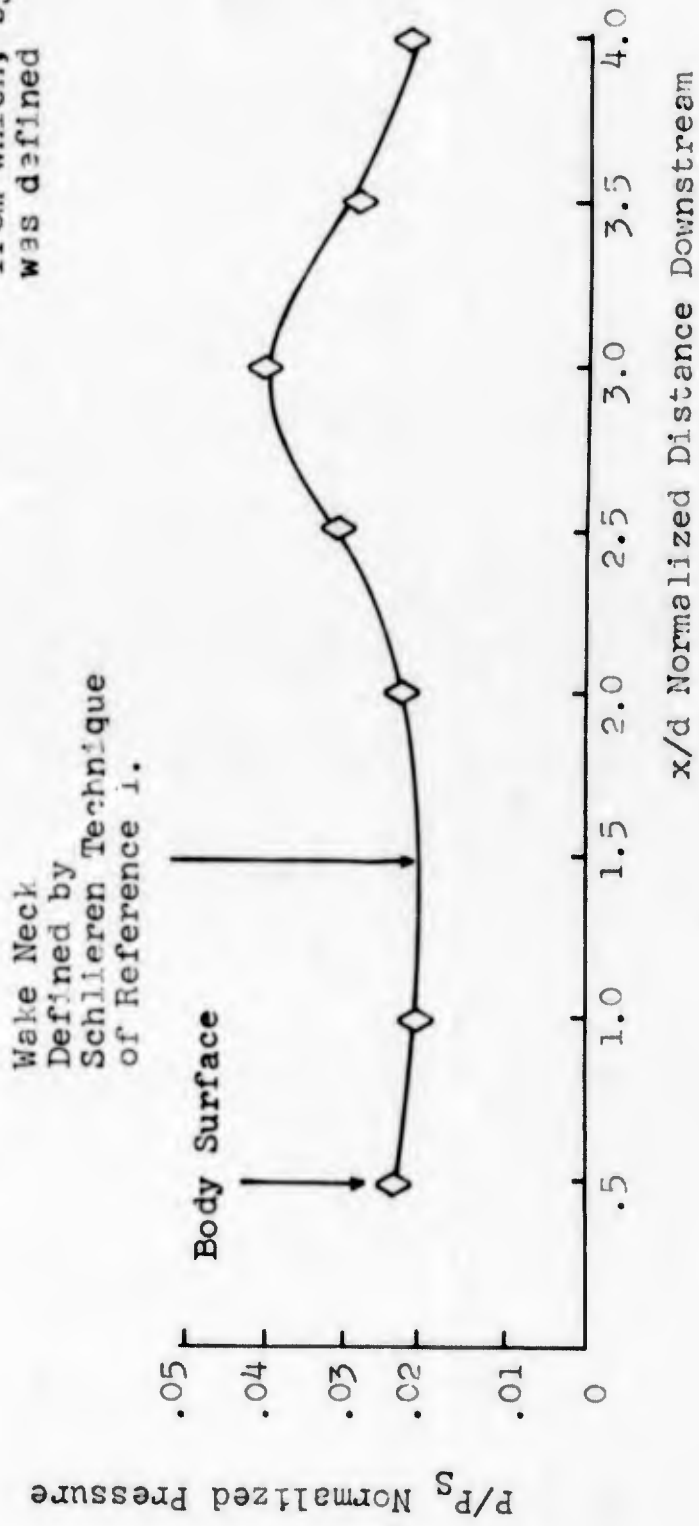


FIGURE 10 - CENTERLINE PRESSURE VARIATION DOWNSTREAM OF THE MODEL

α (Angle of Probe)



Rearward Facing Probe Pressure Profile from which, by symmetry, the centerline was defined



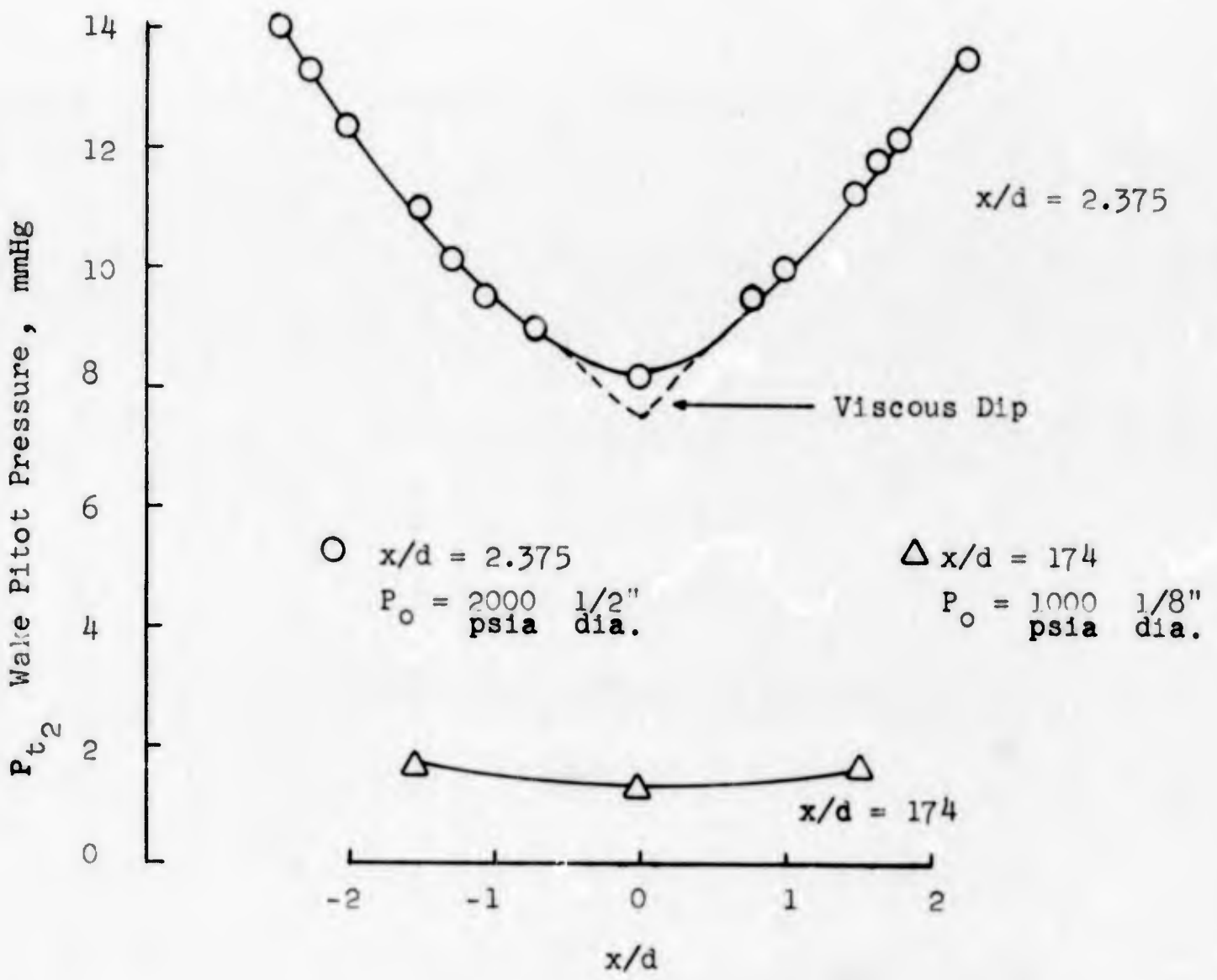


FIGURE 11 - PITOT PRESSURE PROFILES IN NEAR AND FAR WAKE

Hot Wire : .0001" dia., Pt - 90%Pt10%Pd

Elect. Resistance; $R_o = 10.70\text{ohm}$ at 85°F

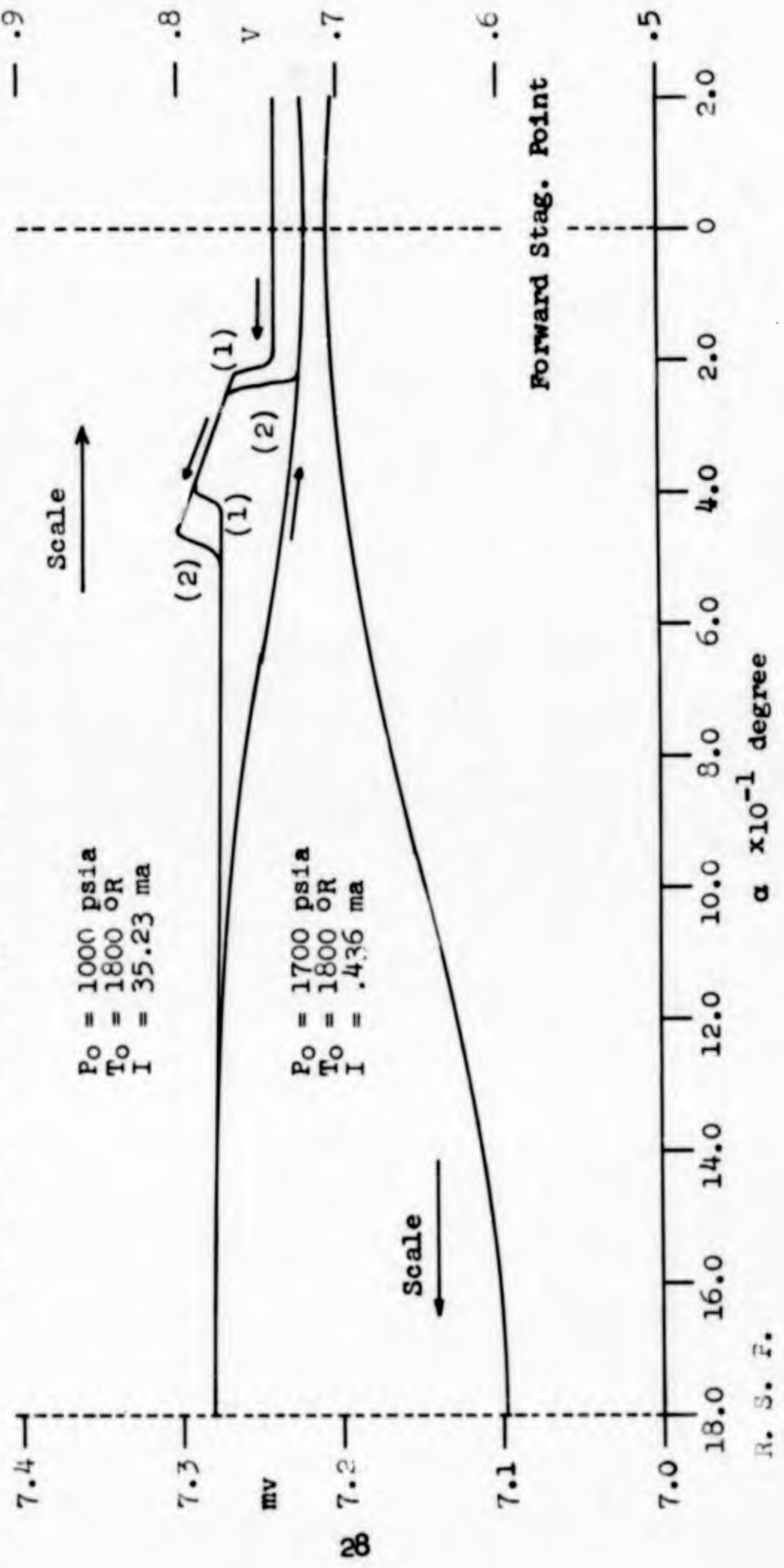


FIGURE 12 - HOT WIRE ANEMOMETER RESULT

Unclassified

Security Classification

DOCUMENT CONTROL DATA - R&D		
<i>(Security classification of title, body of abstract and indexing annotation must be entered when the overall report is classified)</i>		
1. ORIGINATING ACTIVITY (Corporate author) University of Cincinnati College of Engineering Cincinnati, Ohio 45221		2a. REPORT SECURITY CLASSIFICATION Unclassified
		2b. GROUP
3. REPORT TITLE Experimental Investigations of Hypersonic Flow Around Two Dimensional Circular Cylinders		
4. DESCRIPTIVE NOTES (Type of report and inclusive dates) Interim Oct to June 1964		
5. AUTHOR(S) (Last name, first name, initial) K. H. Token and H. Oguro		
6. REPORT DATE October 1965	7a. TOTAL NO. OF PAGES 28	7b. NO. OF REFS 2
8a. CONTRACT OR GRANT NO. AF 33(616)-8453	9a. ORIGINATOR'S REPORT NUMBER(S)	
b. PROJECT NO. 7064		
c. 61445014	9b. OTHER REPORT NO(S) (Any other numbers that may be assigned this report)	
d. 681307	ARL 65-212	
10. AVAILABILITY/LIMITATION NOTICES Qualified requesters may obtain copies from DDC. Released to OTS.		
11. SUPPLEMENTARY NOTES	12. SPONSORING MILITARY ACTIVITY Aerospace Research Laboratories (ARR) Office of Aerospace Research, USAF Wright-Patterson AFB, Ohio	
13. ABSTRACT This paper describes an experimental investigation of the flow phenomena about a two-dimensional circular cylinder in a hypersonic stream. The purpose of the investigation was to record properties of the flow regions which have a direct effect on the wake behind a two-dimensional circular cylinder. All data were obtained at a nominal Mach number of 14 and a stagnation temperature of 1800°R. The total pressure settings were between 600 and 2000 psia, although the majority of the data was taken at 1000, 1200, 1400, or 1600 psia. Model diameters varied from 1/4 to 3/4 to 3/4 inch, however tests about 3/8 and 1/2 inch diameter models were most common. Data concerning pressure distributions at the body, in the base flow region and near wake were obtained. In addition, some qualitative results were obtained with the hot wire anemometer at the body surface.		

DD FORM 1473
1 JAN 64

Unclassified

Security Classification

14. KEY WORDS	LINK A		LINK B		LINK C	
	ROLE	WT	ROLE	WT	ROLE	WT

Hypersonic flow
 Two-dimensional circular cylinders
 High speed flow
 Base flow

INSTRUCTIONS

1. ORIGINATING ACTIVITY: Enter the name and address of the contractor, subcontractor, grantee, Department of Defense activity or other organization (*corporate author*) issuing the report.

2a. REPORT SECURITY CLASSIFICATION: Enter the overall security classification of the report. Indicate whether "Restricted Data" is included. Marking is to be in accordance with appropriate security regulations.

2b. GROUP: Automatic downgrading is specified in DoD Directive 5200.10 and Armed Forces Industrial Manual. Enter the group number. Also, when applicable, show that optional markings have been used for Group 3 and Group 4 as authorized.

3. REPORT TITLE: Enter the complete report title in capital letters. Titles in all cases should be unclassified. If a meaningful title cannot be selected without classification, show title classification in all capitals in parenthesis immediately following the title.

4. DESCRIPTIVE NOTES: If appropriate, enter the type of report, e.g., interim, progress, summary, annual, or final. Give the inclusive dates when a specific reporting period is covered.

5. AUTHOR(S): Enter the name(s) of author(s) as shown on or in the report. Enter last name, first name, middle initial. If military, show rank and branch of service. The name of the principal author is an absolute minimum requirement.

6. REPORT DATE: Enter the date of the report as day, month, year, or month, year. If more than one date appears on the report, use date of publication.

7a. TOTAL NUMBER OF PAGES: The total page count should follow normal pagination procedures, i.e., enter the number of pages containing information.

7b. NUMBER OF REFERENCES: Enter the total number of references cited in the report.

8a. CONTRACT OR GRANT NUMBER: If appropriate, enter the applicable number of the contract or grant under which the report was written.

8b, 8c, & 8d. PROJECT NUMBER: Enter the appropriate military department identification, such as project number, subproject number, system numbers, task number, etc.

9a. ORIGINATOR'S REPORT NUMBER(S): Enter the official report number by which the document will be identified and controlled by the originating activity. This number must be unique to this report.

9b. OTHER REPORT NUMBER(S): If the report has been assigned any other report numbers (*either by the originator or by the sponsor*), also enter this number(s).

10. AVAILABILITY/LIMITATION NOTICES: Enter any limitations on further dissemination of the report, other than those

imposed by security classification, using standard statements such as:

- (1) "Qualified requesters may obtain copies of this report from DDC."
- (2) "Foreign announcement and dissemination of this report by DDC is not authorized."
- (3) "U. S. Government agencies may obtain copies of this report directly from DDC. Other qualified DDC users shall request through _____."
- (4) "U. S. military agencies may obtain copies of this report directly from DDC. Other qualified users shall request through _____."
- (5) "All distribution of this report is controlled. Qualified DDC users shall request through _____."

If the report has been furnished to the Office of Technical Services, Department of Commerce, for sale to the public, indicate this fact and enter the price, if known.

11. SUPPLEMENTARY NOTES: Use for additional explanatory notes.

12. SPONSORING MILITARY ACTIVITY: Enter the name of the departmental project office or laboratory sponsoring (*paying for*) the research and development. Include address.

13. ABSTRACT: Enter an abstract giving a brief and factual summary of the document indicative of the report, even though it may also appear elsewhere in the body of the technical report. If additional space is required, a continuation sheet shall be attached.

It is highly desirable that the abstract of classified reports be unclassified. Each paragraph of the abstract shall end with an indication of the military security classification of the information in the paragraph, represented as (TS), (S), (C), or (U).

There is no limitation on the length of the abstract. However, the suggested length is from 150 to 225 words.

14. KEY WORDS: Key words are technically meaningful terms or short phrases that characterize a report and may be used as index entries for cataloging the report. Key words must be selected so that no security classification is required. Identifiers, such as equipment model designation, trade name, military project code name, geographic location, may be used as key words but will be followed by an indication of technical context. The assignment of links, rules, and weights is optional.